Composites Part B 222 (2021) 109072

Contents lists available at ScienceDirect

Composites Part B

journal homepage: www.elsevier.com/locate/compositesb

Nano-bridge effect on thermal conductivity of hybrid polymer composites incorporating 1D and 2D nanocarbon fillers

Ji-un Jang [a], Seung Hwan Lee [b], Jaewoo Kim [c], Seong Yun Kim [b,*], Seong Hun Kim [a,**]

[a] Department of Organic and Nano Engineering, Hanyang University, 222 Wangsimni-ro, Haengdang-dong, Seongdong-gu, Seoul, 04763, Republic of Korea
[b] Department of Organic Materials and Textile Engineering, Jeonbuk National University, 567 Baekje-daero, Deokjin-gu, Jeonju-si, Jeonbuk, 54896, Republic of Korea
[c] Composite Materials Applications Research Center, Institute of Advanced Composite Materials, Korea Institute of Science and Technology (KIST), 92 Chudong-ro, Bongdong-eup, Wanju-gun, Jeonbuk, 55324, Republic of Korea

ARTICLE INFO

Keywords:
Polymer-matrix composites (PMCs)
Particle-reinforcement
Thermal properties
Analytical modelling
Thermal analysis

ABSTRACT

Numerous studies have been reported on thermal interface materials based on synergistic hybrid effects, however, most of them contain only fragmentary experimental results and the related model has been rarely proposed to explain the effects exactly. Herein, the thermal conductivities of the composites were systematically evaluated according to various filler contents and ratios. It was found that the fraction of the secondary filler inducing the maximum synergistic effect decreased as the total filler content increased. In addition, when the fraction was higher than the optimum fraction, the anti-synergistic effect occurred. At the optimum fraction, effective phonon transfer was induced due to the improved filler network formation of graphene nanoplatelet (GNP)-carbon nanotube (CNT), thereby achieving high thermal conductivity of 7.69 W/m·K at $f_{GNP} = 27.69$ vol% and $f_{CNT} = 0.57$ vol%. Moreover, the Kim-Jang-Lee (KJL) model for the synergistic effect was proposed by introducing filler-ratio variables into the critical percolation equation reported previously, and the KJL model for the anti-synergistic effect was proposed based on the rule of mixture of composites filled with the optimal connected filler network and filled with the excessive secondary filler.

1. Introduction

Implementing the excellent conductive properties of carbon nanotube (CNT, electrical conductivity of 10^3–10^5 S/cm and thermal conductivity of 3000 W/m·K) [1–4] and graphene (electron mobility of 200,000 cm^2/V·s and thermal conductivity of 3000–5150 W/m·K) [5–7] into applied products through a low-cost process is one of the most important issues in nano-engineering science. Numerous studies related to polymer nanocomposites have been conducted because of the combined advantage of not only being able to fabricate handable intermediate materials but also providing excellent conductivity of nanocarbons to polymer materials exhibiting insulating properties [8–12]. It had been reported that the electrical conductivity of polymer nanocomposite showed an innovative increase with the introduction of the nanocarbon fillers, while the improvement of the thermal conductivity showed a relatively slight and linear increase. It is well established that the electrical conductivity of nanocarbon composites is improved based on the percolation theory including electron tunneling effects. On the other hand, the thermal conductivity of nanocarbon composites is known to be based on phonon transfer governed by interfacial thermal resistance (ITR) between nanocarbon and polymer matrix, and contact thermal resistance (CTR) between nanocarbon fillers. However, the thermal conduction mechanism of the nanocarbon composite material has an issue that has not yet been clearly identified compared to the electrical conduction mechanism.

Important discoveries regarding the thermal conductivity of nano-based composites have been reported until recently [11–13]. When nanofillers are incorporated into the polymer matrix, the interfacial portion increases due to the large specific surface area of the filler. This results in high ITR owing to scattering of phonons by lattice mismatches of dissimilar materials [14–16]. As a result, thermal conductivities near the lower boundary of the rule of mixture (ROM) have been reported mostly [14]. To obtain a higher thermal conductivity, some studies attempted to connect the fillers inside the highly loaded nanocomposite material, and reported thermal percolation behavior [17,18]. However, this method is only applicable to certain highly loaded nanocomposites.

* Corresponding author.
** Corresponding author.
E-mail addresses: sykim82@jbnu.ac.kr (S.Y. Kim), kimsh@hanyang.ac.kr (S.H. Kim).

https://doi.org/10.1016/j.compositesb.2021.109072
Received 3 March 2021; Received in revised form 13 May 2021; Accepted 6 June 2021
Available online 9 June 2021

Alternatively, a hybrid technique was proposed in which a one-dimensional (1D) filler as a secondary filler was incorporated to form a heat conduction network [19,20]. The added 1D nanofillers formed the connected filler network, converting the heat conduction mechanism dominated by ITR (8×10^{-8} to 2×10^{-7} m^2K/W) to that dominated by CTR ($\sim 3.05 \times 10^{-9}$ m^2K/W) [21,22]. Numerous studies [15,19,23] have previously reported an enhancement in thermal conductivity of composite materials, based on a synergistic effect in hybrid filler systems, however, most of them reported fragmentary experimental results on hybrid effects. Yu et al. [19] experimentally investigated the content and ratio of a hybrid filler system comprised of graphene nanoplatelet (GNP) and CNT. A synergistic increase in thermal conductivity at low filler loadings was reported, and the nano-bridges of 1D CNTs formed between two-dimensional (2D) GNPs caused the synergistic increase in the thermal conductivity of composites with heterogeneous fillers. They also reported for the first time an anti-synergistic effect on the reduction of the thermal conductivity at high filler loadings. However, the optimal filler content and ratio, and the reason for the generation of the anti-synergistic effect have not been clearly identified.

This study deals with the following issues that have not been clearly addressed in the thermal conductivity of polymer nanocomposites incorporating 1D and 2D fillers. i) Although many studies have reported the simple observations that the thermal conductivity of composite materials increases synergistically based on a hybrid filler system, the synergistic effect and behavior have not been fully understood due to the lack of systematic experimental results. ii) The anti-synergistic effect reported previously [19] has not been clearly identified. iii) It is necessary to propose a theoretical model that can explain these synergistic and anti-synergistic effects of polymer composites incorporating hybrid fillers. In order to solve these issues, the thermal conductivity of the nanocomposite containing multi-walled CNT (MWCNT) and GNP in various ratios (MWCNT to GNP volume ratio of 0–1) up to 37.14 vol% was systematically analyzed. The synergistic increase based on the nano-bridge effect as well as the mechanism of the anti-synergistic effect, in the thermal conductivity, was identified. In addition, the Kim-Jang-Lee (KJL) model that can explain the synergistic improvement considering the nano-bridge effect, and anti-synergistic effect was proposed.

2. Experimental

2.1. Materials

2D GNP (M25, XG Science Co., Lansing, MI, USA) with the lateral size of 25 μm and the thickness of 5–10 nm [24], was applied as the primary filler for improving the thermal conductivity of the composites as shown in Fig. S1a. MWCNT (Jenotube 8, JEIO Co., Incheon, Korea) was adopted as the secondary filler with the bundle length of 100–200 μm and the single strand thickness of 7–10 nm as shown in Figs. S1b and c [25]. The cyclic butylene terephthalate (CBT, CBT 160, Cyclics Co., Schenectady, NY, USA) oligomer resin was used as the matrix.

2.2. Fabrication

As shown in Fig. S2, GNP and MWCNT dried at 80 °C for 12 h were powder-mixed with milled CBT at 2000 rpm for 4 min and then the mixture was transferred to a metallic mold (25 mm × 25 mm × 2 mm) [26]. The CBT matrix of the mixture was *in situ* polymerized for 20 min at 230 °C and 15 MPa using a hot-press (Dae Heung Science Co., Incheon, Korea). During the process, CBT of low molecular weight (Mw = 220 × n g/mol) composed of butyl monomers (n = 2–7) melted above 130 °C, and the nanocarbon fillers could be well-dispersed due to its low viscosity (~0.02 pa·s) [25,26]. At temperature above 160 °C, CBT could be ring-opening polymerized by a tin-based catalyst (butyltin chloride dihydroxide, FASCAT 4101, Arkema GmbH, Düsseldorf, Germany) of 3 mol‰ and exhibited a molecular structure similar to that of linear poly (butylene terephthalate) (PBT). The compositions of the fabricated nanocomposites are listed in Table 1.

2.3. Characterization

Fourier transform infrared (FT-IR) spectroscopy, Raman spectroscopy and X-ray photoelectron spectroscopy (XPS) results of GNP and

Table 1
Compositions of the fabricated composites.

Sample	Matrix content (vol%)	Filler content (vol%)	GNP content (vol%)	MWCNT content (vol%)	MWCNT to GNP vol. ratio (ψ)
pCBT	100	–	–	–	–
pCBT/GNP	93.84	6.16	6.16	–	0
	90.56	9.44	9.44	–	0
	79.79	20.21	20.21	–	0
	71.74	28.26	28.26	–	0
	65.00	35.00	35.00	–	0
	62.86	37.14	37.14	–	0
pCBT/ MWCNT	93.84	6.16	–	6.16	1
	90.56	9.44	–	9.44	1
	79.79	20.21	–	20.21	1
	71.74	28.26	–	28.26	1
	62.86	37.14	–	37.14	1
pCBT/GNP/ MWCNT	93.84	6.16	6.10	0.06	0.01
			6.04	0.12	0.02
			5.85	0.31	0.05
			5.54	0.62	0.1
			4.93	1.23	0.2
			3.70	2.46	0.4
			2.46	3.70	0.6
			1.23	4.93	0.8
	90.56	9.44	9.35	0.09	0.01
			9.25	0.19	0.02
			8.97	0.47	0.05
			8.78	0.66	0.07
			8.50	0.94	0.1
			7.55	1.89	0.2
			5.66	3.78	0.4
			3.78	5.66	0.6
			1.89	7.55	0.8
	79.79	20.21	20.01	0.20	0.01
			19.81	0.40	0.02
			19.20	1.01	0.05
			18.19	2.02	0.1
			16.17	4.04	0.2
			12.13	8.08	0.4
			8.08	12.13	0.6
			4.04	16.17	0.8
	71.74	28.26	27.98	0.28	0.01
			27.69	0.57	0.02
			26.85	1.41	0.05
			25.43	2.83	0.1
			22.61	5.65	0.2
			16.96	11.30	0.4
			11.30	16.96	0.6
			5.65	22.61	0.8
	62.86	37.14	37.10	0.04	0.001
			36.95	0.19	0.005
			36.77	0.37	0.01
			36.40	0.74	0.02
			35.28	1.86	0.05
			33.43	3.71	0.1
			29.71	7.43	0.2
			22.28	14.86	0.4
			14.86	22.28	0.6
			7.43	29.71	0.8
[a]pCBT/GNP/ MWCNT (MWCNT add.)	62.83	37.17	37.14	0.03	0.001
	62.67	37.33	37.14	0.19	0.005
	62.49	37.51	37.14	0.37	0.01

[a] MWCNT add. indicated the small amounts of MWCNT added to the pCBT/GNP 37.14 vol% composite.

MWCNT are shown in Figs. S1d–f and the defect levels of GNP and MWCNT were 0.28 and 1.38, respectively (supporting characterization in Section S1.1 of Supplementary data). The isotropic thermal conductivity of the prepared samples (25 mm × 25 mm × 2 mm) was measured according to the ISO 22007-2 standard using a thermal conductivity analyzer (TPS 2500 S, Hot disk AB, Gothenburg, Sweden). To investigate internal structures inside the fabricated specimens, the composite samples were fractured after freezing in liquid nitrogen. the fractured surfaces of the composites were observed under a voltage of 10 kV using a field emission scanning electron microscope (FE-SEM, SUPRA 40 VP, Carl Zeiss, Oberkochen, Germany) after they were coated with Pt for 100 s under vacuum by a coating machine (EM ACE 200, Leica Microsystems, Wetzar, Germany). In addition, high-magnification fracture surface analysis was performed using an aberration-corrected scanning transmission electron microscopy (STEM, JEM-ARM200F, JEOL, Tokyo, Japan). The specimens were milled using a focused (Ga) ion beam (FIB, JIB-4601F, JEOL, Tokyo, Japan), and then they were placed on a grid and observed at a voltage of 80 kV. Non-destructive three-dimensional (3D) analysis was performed via micro-computed tomography (μ-CT, Skyscan 1172, Bruker Co., Billerica, MA, USA) to obtain the topological images in a wide-area (~1 mm^3) of the specimen. The raw images obtained by radiation of X-rays (10 kV) were reconstructed into 2D images, and then the 2D images were integrated into a 3D image using a software. Thermal images for practical thermal interface materials (TIMs) application were obtained using an infrared (IR) thermal camera (FLIR-T62101, FLIR Systems Inc., Wilsonville, OR, USA) with a resolution of 0.02 K. The temperature of the prepared specimen was measured at 5 s after placing on a central processing unit (CPU) (97 °C) of a powered personal computer at an atmospheric temperature of 24 °C (additional characterizations in Section S1.2-1.3 of Supplementary data).

3. Results and discussion

To systematically obtain experimental results, the fillers should be uniformly dispersed over the evaluated filler loading. In the present study, the solvent-free melting process proposed in the previous study was applied [26], as shown in Fig. S2. By using the applied method, the fillers were easily mixed even at high contents (~37.14 vol%) because of the low melt-viscosity (~0.02 Pa s) of the CBT oligomer resin. Further, the fillers could be uniformly dispersed by physical mixing at a high-speed rotation (2000 rpm) and by the *in situ* polymerization of oligomer resin [26,27]. Under ambient atmosphere with a relative humidity of 60% and at temperature above 160 °C, CBT molecules are ring-opening polymerized to become the polymerized CBT (pCBT) similar to that of linear PBT. pCBT exhibits a tensile strength of 57 MPa [28]. Additional results and discussion on the polymerization of the CBT matrix are provided in Section S2 and Fig. S3 of Supplementary data [25, 29].

3.1. Thermal percolation behavior

The thermal conductivity of the prepared composite is shown in Fig. 1. As shown in Fig. 1a, when the GNP composition was 28.26 vol%, the thermal conductivity increased by 2275% (4.75 W/m·K), compared to that of the control group (0.2 W/m·K, the thermal conductivity of pCBT). The thermal conductivities calculated based on Nan's equation (see Section S3.1 of Supplementary data) were in accordance with the experimental results [30], showing the typical linear trend. Nan's model

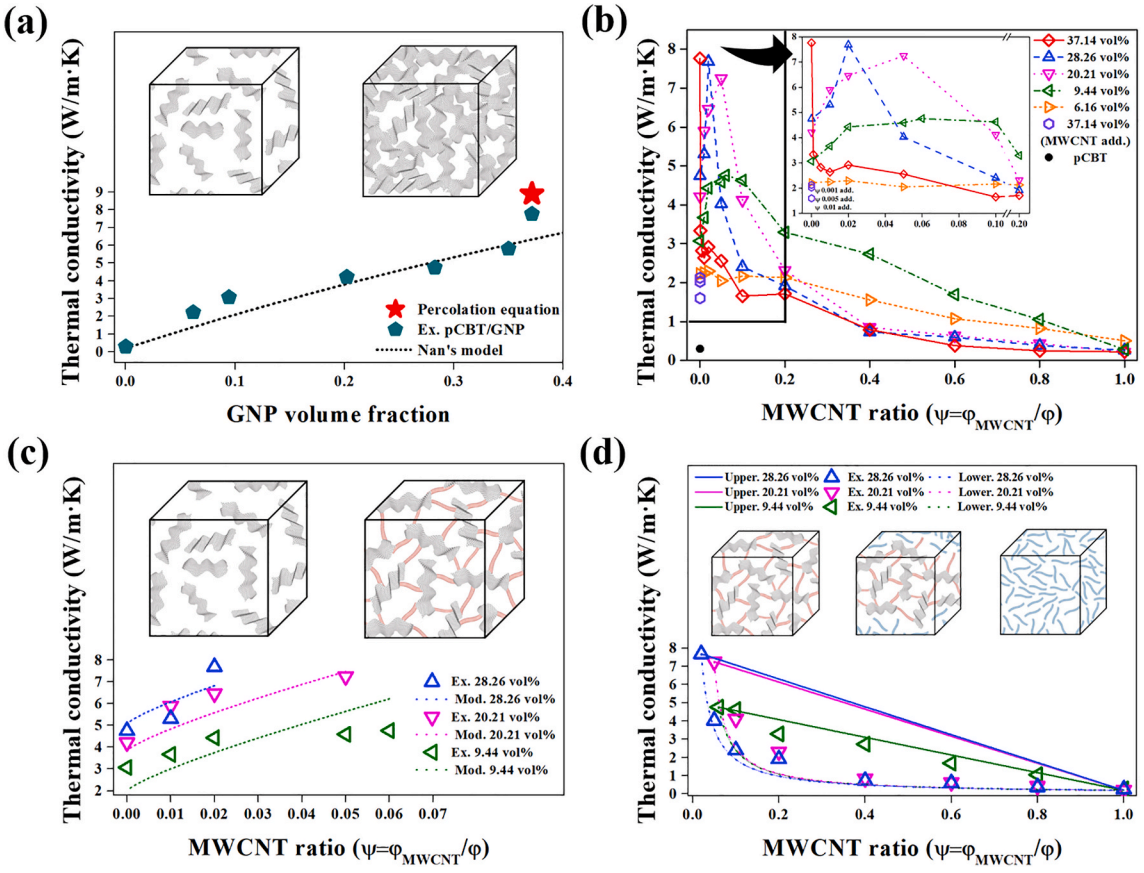

Fig. 1. Thermal conductivity of composites incorporated with (a) primary filler (GNP) according to volume fraction (vol%) (inset image: schematic of nano-bridges of GNPs), (b) GNP/MWCNT heterogeneous fillers according to MWCNT ratio (ψ) (inset image: thermal conductivity according to ψ in the range of 0–0.2), (c) GNP/MWCNT according to MWCNT ratio (ψ) ($0 < \psi < \psi_M$) (inset image: schematic of nano-bridges of GNPs-MWCNTs), and (d) GNP/MWCNT according to MWCNT ratio (ψ) ($\psi > \psi_M$) (inset image: schematic of anti-synergistic effect).

assumes random filler dispersion of the composite, implying that the incorporated GNP particles were uniformly dispersed and mixed in an uncontacted form. However, the composite with 37.14 vol% GNP exhibited a remarkable enhancement in the thermal conductivity (7.76 W/m·K, which increased by 3780% compared to that of the control), which occurred at a much higher level than the theoretical value from Nan's equation. This could be explained by the thermal percolation generated by direct contacts between the fillers [17,18]. Such remarkable enhancement was well explained by the critical percolation equation (see Section S3.2 of Supplementary data) with a critical exponent of 0.84 [17,18,31]. Table 2 summarizes the thermal conductivities of composites with graphene-based fillers reported in previous studies [19,23,32–49], and we achieved 7.76 W/m·K (the best result to the best of our knowledge), which meant it increased by 3780% in comparison with the polymer's thermal conductivity. Therefore, the thermal conductivity of the composite filled with the primary filler increased linearly with the GNP content, when direct contacts between the fillers occurred (schematic of Fig. 1a), the thermal conductivity rapidly increased due to the formation of nano-bridges within the composite.

To explain further the thermal percolation behavior due to direct contacts between GNP fillers, the morphological images of the fabricated pCBT/GNP composites are shown in Fig. 2a–d. Connected GNP fillers were rarely observed in the composite with 28.26 vol% GNP, while nano-bridges, the connected structures of GNP fillers, were clearly found in the composite with 37.14 vol% GNP. Furthermore, it was double-checked that the connected filler structure in the composite with 28.26 vol% GNP hardly occurred, as shown in the non-destructive internal observation (Fig. 2e and f) using μ-CT. However, at 37.14 vol% GNP, nano-bridges between the connected fillers were clearly observed (Fig. 2g and h) (see Supplementary video), which were consistent with the morphological results. Therefore, the thermal conductivity of composites with the connected filler network formed by nano-bridges remarkably increased by switching the high level of phonon scattering based on the ITR between the matrix and fillers to the relatively low level of that based on the CTR between the connected fillers.

Table 2
Thermal conductivity of composites with graphene-based fillers.

Filler type	Thermal conductivity (W/m·K)	Enhancement (%)	Loading	Matrix	Ref.
GNP	7.76	3780	37.14 vol%	pCBT	This work
GNP	~7.00	~3400	40 wt%	Epoxy	[23]
GNP	~7.00	~3383	40 wt%	Epoxy	[19]
GNP	6.44	3104	25 vol%	Epoxy	[32]
GNP	~6.00	~2900	50 vol%	Epoxy	[33]
EG[a)]	~2.70	~514	~25 wt %	HDPE[b)]	[34]
GNP	1.64	613	20 wt%	PVDF[c)]	[35]
GNP	1.61	455	4 wt%	PEG[d)]	[36]
GNP	0.97	223	5 wt%	PVDF/PMMA[e)]	[37]
GNP	0.72	240	2.7 vol%	Epoxy	[38]
GNP	0.70	37	1.3 vol%	TATB[f)]	[39]
MGF[g)]	0.60	200	2.7 vol%	PDMS[h)]	[40]
GNP	0.60	95	1 wt%	PEG	[41]
GNP	0.52	49	0.5 wt%	EPO[i)]	[42]
GNP	0.50	200	8 wt%	Epoxy	[43]
GNP	~0.47	~115	5 wt%	Epoxy	[44]
GNP	0.36	80	4 wt%	PDMS	[45]
RGO[j)]	0.30	50	1 wt%	PP[k)]	[46]
GO[l)]	0.29	32	10 wt%	PVDF	[47]
GNP	~0.27	~22	0.5 wt%	PEI[m)]	[48]
GNP	0.16	24	1.0 wt%	Epoxy	[49]

[a)]Expanded graphite; [b)]High density polyethylene; [c)]Poly (vinylidene flouride); [d)]Polyethylene glycol; [e)]Poly (methyl methacrylate); [f)]1,3,5-triamino-2,4,6-trinitrobenzene; [g)]multylayer graphene flake; [h)]polydimethylsiloxane; [i)]Expanded perlite; [j)]Reduced graphene oxide; [k)]Polypropylene; [l)]Graphene oxide; [m)]Polyetherimide.

3.2. Synergistic and anti-synergistic effects

The thermal conductivities of the pCBT/GNP/MWCNT composites in terms of filler loading and secondary filler ratio (ψ) are shown in Fig. 1b. The thermal conductivity of the composite for each filler content increased to a certain ratio (ψ_M, MWCNT ratio at maximum enhancement of the thermal conductivity for each filler content) and then decreased as ψ increased ($\psi > \psi_M$). The synergistic and anti-synergistic behaviors were clearly confirmed at filler contents in the range of 9.44–28.26 vol% as shown in the inset image of Fig. 1b. It was confirmed that ψ_M representing the maximum thermal conductivity of the composite was different for each filler content. The enhanced thermal conductivities of the pCBT/GNP/MWCNT composites of 4.76 (enhancement ≈ 55%, $\psi_M = 0.06$), 7.25 (≈72% $\psi_M = 0.05$) and 7.69 W/m·K (≈62%, $\psi_M = 0.02$) were observed, compared to those of the pCBT/GNP composites of 3.07, 4.22 and 4.76 W/m·K at filler contents of 9.44, 20.21 and 28.26 vol%, respectively. These results indicated that the nano-bridges were optimized at ψ_M for phonon transfer. As the total filler content increased, the optimum ratio (ψ_M) related to the switching between the synergistic and anti-synergistic effects decreased.

In the synergistic enhancement behavior, the secondary 1D filler acted as the nano-bridge connecting the primary 2D fillers (schematic of Fig. 1c). This resulted in the switch of the thermal conduction mechanism from the system governed by the ITR between filler-resin to that governed by the CTR based on a connected hybrid filler network [21,22]. Table 3 summarizes thermal conductivities of composites with graphene-CNT hybrid fillers reported in previous studies [19,33–35,39,45,46,48–51], which revealed the synergistic effect. In the high-loading composite with GNP and MWCNT fractions of 27.69 and 0.57 vol%, we achieved 7.69 W/m·K (the best result to the best of our knowledge), which meant it increased by 3745% in comparison with the polymer's thermal conductivity. In contrast, the anti-synergistic effect, defined as a decrease in thermal conductivity as ψ increased ($\psi > \psi_M$), was originated from the incorporation of an additional secondary filler after the primary (GNP)-secondary (MWCNT) connection structure was formed at ψ_M (shown in schematic of Fig. 1d). This indicated that the anti-synergistic effect was caused by the increase of the ITR due to an excessive 1D filler which could not act as the nano-bridge.

Fig. 3a–d and Figs. S4a–h show the morphological images of pCBT/GNP/MWCNT composites with filler content at the optimal thermal conductivities, explaining the presence of nano-bridges between the GNP and MWCNT fillers. Connected GNP-MWCNT network was clearly observed, indicating that the secondary filler could promote phonon transfer via nano-bridge formation. In particular, as shown in Fig. 3d, MWCNTs overlaid on the GNPs were observed using STEM at a high magnification of the fracture sheet of the pCBT/GNP/MWCNT composite (28.26 vol%, $\psi = 0.02$). It was confirmed that the formed bridges were nanoscale. 3D internal structure of a large-area composite (~1 mm^3) analyzed using μ-CT is shown in Fig. 3e–h, Figs. S4i and j. Despite the same filler loading (28.26 vol%), MWCNT bridges (red color) formed better between GNPs (blue color) when the MWCNT ratio (ψ) was 0.02 (see Supplementary video) and the excessive MWCNT fillers were confirmed when the MWCNT ratio (ψ) was 0.10. Therefore, it was confirmed that the incorporation of the secondary filler exceeding the optimum ratio (ψ_M) could not play a role in the nano-bridge, resulting in the anti-synergistic effect on the thermal conductivity.

In the case based on the composite containing 37.14 vol% GNP (the thermal conductivity of 7.76 W/m·K), thermal conductivities (1.65–3.34 W/m·K) of the composites in which some GNP contents were substituted for the secondary MWCNT fillers were considerably reduced as shown in the inset image of Fig. 1b. In particular, for the composites in which the secondary filler was additionally incorporated, the thermal conductivities (1.60–2.13 W/m·K) also decreased rapidly (MWCNT add. of inset image in Fig. 1b). These results indicated that the connected

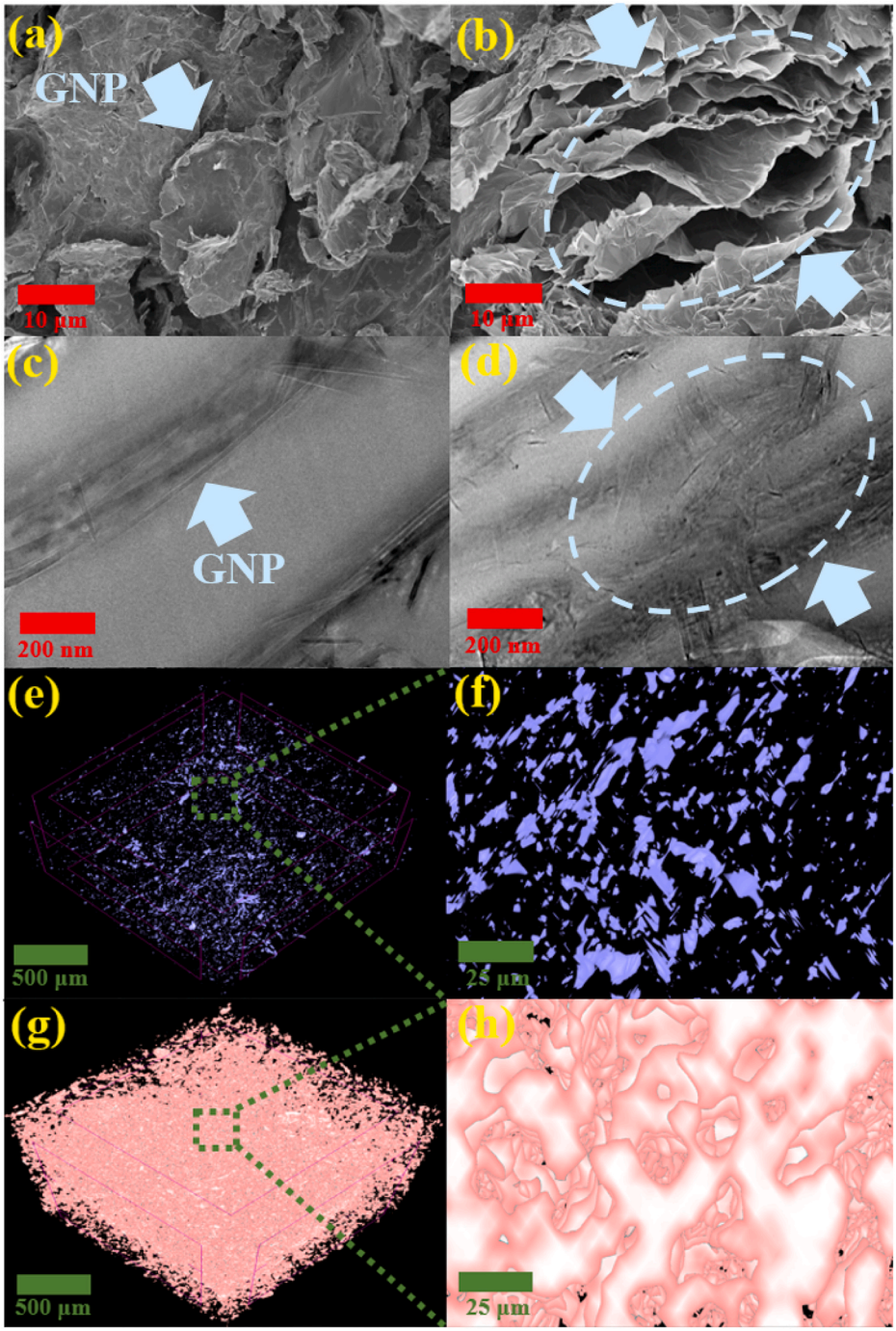

Fig. 2. FE-SEM images of composites with (a) 28.26 vol% GNP and (b) 37.14 vol% GNP. STEM images of composites with (c) 28.26 vol% GNP and (d) 37.14 vol% GNP. μ-CT images of composites filled with 28.26 vol% GNP in (e) low magnification and (f) high magnification, and 37.14 vol% GNP in (g) low magnification and (h) high magnification.

GNP network was the optimal structure for improving the thermal conductivity of the composites. When the secondary filler replaced some content of the primary filler, the reduced thermal conductivity could be explained by the increased CTR due to the reduced contact area between the fillers (from GNP-GNP to GNP-MWCNT). In the case where the secondary filler was further added, the incorporated MWCNTs acted as the excessive secondary filler, inducing extra MWCNT-polymer ITR.

3.3. Nano-bridge effect

This study reported the synergistic and anti-synergistic thermal conductivity enhancement behaviors that could not be simulated by the Nan's and percolation equations previously developed based on the conventional material physics. In addition, few theories that could explain these behaviors have been reported. Therefore, a new model was suggested to theoretically explain the hybrid effects.

3.3.1. KJL model for the synergistic hybrid effect

The theoretical prediction based on the synergistic effect of nano-bridges was applied via modification of the previous percolation equation (Eqn. S(4) of Section S2). The term $TC_m \times (1-\varphi_G)$ was converted to TC_N calculated based on Nan's model, and the terms φ_G and φ_c were

Table 3
Thermal conductivity of composites with graphene-CNT hybrid fillers.

Filler type	Thermal conductivity (W/m·K)	Enhancement (vs. matrix, %)	Enhancement (vs. single filler, %)	Loading (Graphene + CNT)	Matrix	Ref.
GNP/MWCNT	7.69	3745	62	28.26 (27.69 + 0.57) vol%	pCBT	This work
	7.25	3525	72	20.21 (19.20 + 1.01) vol%		
GNP/MWCNT (GO→GNP, acid treatment)	~7.30	~3550	~21	50 (25 + 25) vol%	Epoxy	[33]
GNP/SWCNT[a)]	~5.00	~2388	~ −28	40 (30 + 10) wt%	Epoxy	[19]
	3.35	1567	~20	20 (15 + 5) wt%		
GO/MWCNT (acid treatment)	~4.40	2100	~44	~50.36 (50 + 0.36) wt %	Epoxy	[50]
EG/MWCNT (heat treatment, 350 °C)	~3.50	~695	~59	25 (20 + 5) wt%	HDPE	[34]
GNP/MWCNT	1.92	735	17	20 (20 + 2) wt%	PVDF	[35]
GNP/MWCNT	1.41	176	104	1.31 (1.179 + 0.131) vol%	TATB	[39]
GNP/MWCNT	1.39	479	23	20 (18 + 2) wt%	PC[b)]	[51]
GNP/MWCNT	0.39	95	9	4 (3 + 1) wt%	PDMS	[45]
RGO/MWCNT	0.35	75	14	1 (0.5 + 0.5) wt%	PP	[46]
GNP/MWCNT	0.32	147	24	1.0 (0.9 + 0.1) wt%	Epoxy	[49]
GNP/MWCNT	~0.33	~50	22	0.5 (0.25 + 0.25) wt%	PEI	[48]

a) Single-walled CNT.
b) Polycarbonate.

replaced with ψ (MWCNT ratio, $\frac{\varphi_{MWCNT}}{\varphi}$) and ψ_c, respectively, because the synergistic effect was due to the connection of the filler structure as the primary filler switched to the secondary filler. Upon substitution of the modified terms, the thermal conductivity based on the nano-bridge effect is expressed as follows:

$$TC_{KJL} = TC_N + TC_i \times \left(\frac{\psi - \psi_c}{1 - \psi_c}\right)^s \quad (\psi < \psi_M) \tag{1}$$

In addition, the critical filler ratio variable (ψ_c) was assumed to be 0 because the introduction of the secondary filler improved the filler connection structure and synergistic thermal conductivity until optimum ratio (ψ_M) was achieved.

$$TC_{KJL} = TC_N + TC_i \times (\psi)^s \quad (\psi < \psi_M) \tag{2}$$

where TC_i and s were the pre-exponential factor (40 W/m·K) and critical exponent (0.8), respectively. The thermal conductivity of the composite according to the change of parameters (TC_i of 30–70 and s of 0.7–0.9) is shown in Fig. S5. The results of the suggested model and the experimental values for the thermal conductivity are shown in Fig. 1c. It was confirmed that those results were in good agreement, indicating that the secondary filler ratio (ψ) is the most important and effective parameter in determing the synergistic effect and thermal conductivitiy at the region ($0 < \psi < \psi_M$).

3.3.2. KJL model for anti-synergistic hybrid effect

The anti-synergistic effect was caused by the generation of a region that contained only excessive secondary filler, in addition to the optimal connected structure of the primary and secondary hybrid filler systems as shown in Fig. 1d. Therefore, it was explained by the ROM of composites filled with only the connected filler network and excessive secondary filler (the typical ROM in Section S3.3 of Supplementary data). The modified ROM (KJL model for anti-synergistic hybrid effect) was suggested upon conversion of the parameters of filler content to those of the MWCNT ratio (ψ). The upper and lower models are suggested as follows:

$$TC_{KJL} = \left[\frac{\frac{1-\psi}{1-\psi_M}}{TC_M} + \frac{\frac{\psi-\psi_M}{1-\psi_M}}{TC_{MWCNT}}\right]^{-1} \quad \text{(lower boundary)} \tag{3}$$

$$TC_{KJL} = \left(\frac{1-\psi}{1-\psi_M}\right) \times TC_M + \left(\frac{\psi-\psi_M}{1-\psi_M}\right) \times TC_{MWCNT} \text{ (upper boundary) } (\psi > \psi_M) \tag{4}$$

where TC_{MWCNT} is thermal conductivity of the pCBT/MWCNT composite ($\psi = 1$) and TC_M is thermal conductivity of pCBT/GNP/MWCNT at ψ_M. As shown in Fig. 1d, the results of the suggested model agreed well with the experimental results. Interestingly, as observed in the conventional ROM [14,52], in this study, when the total filler content of the composite was low (9.44 vol%), the thermal conductivity result was close to the upper boundary, and in the opposite cases (20.21 and 28.26 vol%), the thermal conductivity was close to the lower boundary. The suggested model describing the synergistic and anti-synergistic effects was named the KJL model. This was the core model to explain the nano-bridge effect analyzed and suggested in this study.

3.4. Application

To confirm the heat dissipation characteristics of the fabricated composites as TIMs, thermal images were obtained using an IR camera as shown in Fig. 4. The pCBT specimen (Fig. 4c) placed on the 97 °C CPU showed the lowest heat dissipation due to the thermal conductivity of 0.2 W/m·K. Thermal images of the composites incorporating simultaneously GNP and MWCNT at the contents of 9.44 vol%, 20.21 vol% and 28.26 vol% (Fig. 4d–i) were observed, and a trend was confirmed to coincide with the measured thermal conductivity according to the fraction of the secondary filler (ψ). In addition, in the thermal image of the composite incorporating GNP of 37.14 vol% (Fig. 4j), it was observed that the heat dissipation performance improved due to direct contact between the fillers by showing the specimen temperature 7 °C higher than 28.26 vol% (Fig. 4g). When an additional secondary filler was incorporated in the composite in which the primary filler was mixed at the maximum (Fig. 4h), the reduced heat dissipation performance was confirmed due to the increase of the ITR. It was observed that the temperatures of the specimens on CPU where rapid heat dissipation was required were well accorded with trends of the experimental and theoretical thermal conductivity results. Therefore, it was implied that the optimization of the 3D nano-bridges was an important physical factor for the TIM and the developed KJL model could be applied to practical TIM material design where high thermal conductivity was required.

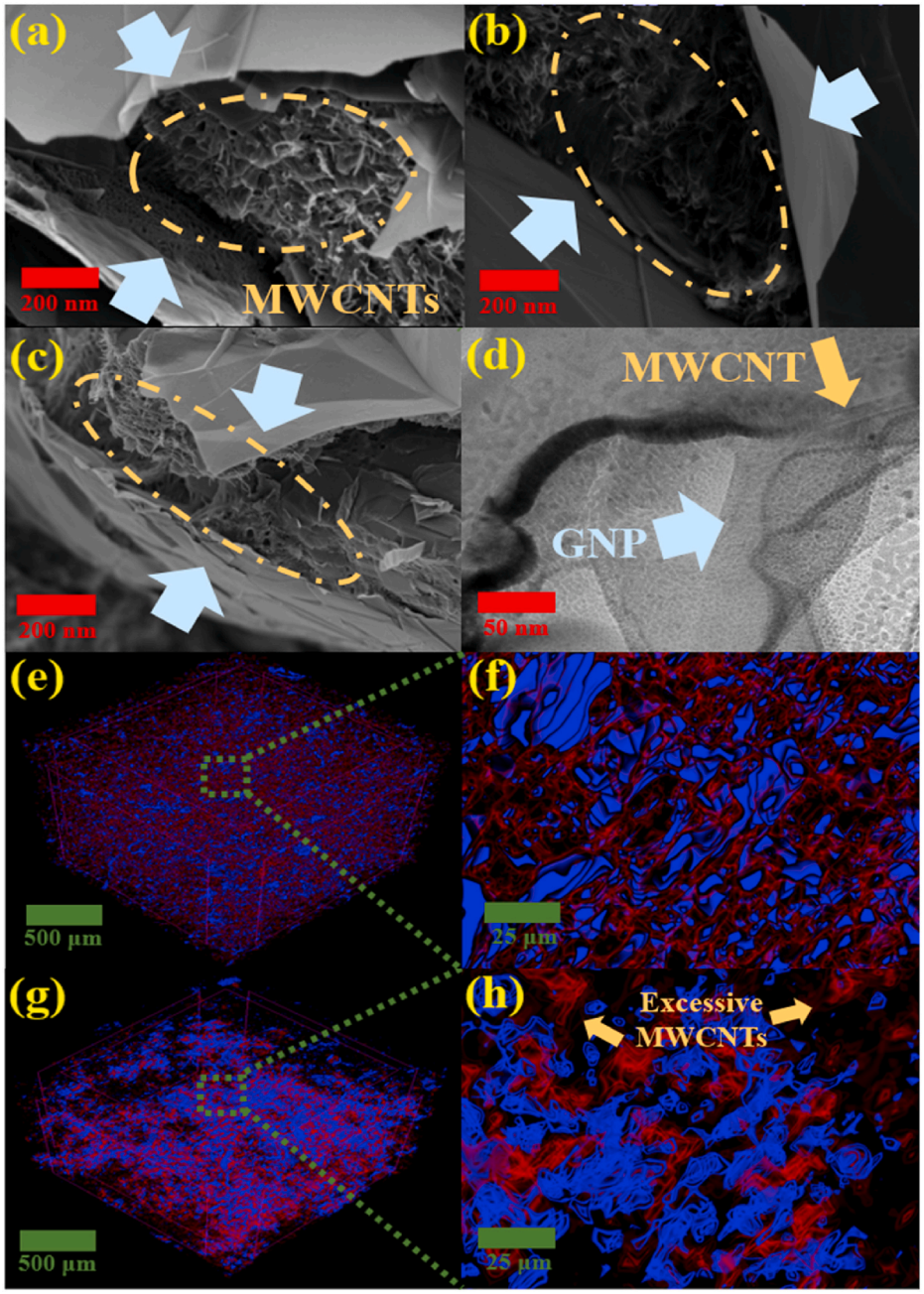

Fig. 3. FE-SEM images of pCBT/GNP/MWCNT composites with (a) 9.44 vol% GNP/MWCNT (ψ = 0.1), (b) 20.21 vol% GNP/MWCNT (ψ = 0.05), and (c) 28.26 vol% GNP/MWCNT (ψ = 0.02). (d) STEM image of composite incorporated with 28.26 vol% GNP/MWCNT (ψ = 0.02). μ-CT images of composites filled with 28.26 vol% GNP/MWCNT (ψ = 0.02), in (e) low magnification and (f) high magnification, and (ψ = 0.10), in (g) low magnification and (h) high magnification (In μ-CT images for hybrid composites, blue and red colors represent GNPs and MWCNTs, respectively). (For interpretation of the references to color in this figure legend, the reader is referred to the Web version of this article.)

4. Conclusion

In many previous studies, fragmentary experimental results have been reported for the synergistic increase in thermal conductivity of composites with hybrid filler systems. In this study, it was found that the proportion of the secondary filler inducing the maximum synergistic effect lowered as the total filler content increased, and the anti-synergistic effect occurred above the optimum fraction. Based on the nano-bridge effect caused by nano-sized connections between fillers, high thermal conductivities of 7.76 and 7.69 W/m·K were achieved for pCBT composites with 37.14 vol% GNP and with the binary fillers of GNP 27.69 vol% and MWCNT 0.57 vol%, respectively. In addition, because it was confirmed that the synergistic increase in the thermal conductivity was due to the connected filler network, the KJL model for the synergistic effect was suggested by introducing filler ratio variables in the critical percolation model. The anti-synergistic effect was attributed to the extra-addition of secondary filler after the optimal construction of the connected filler network. The KJL model for the anti-synergistic effect was also suggested by the modified ROM of the composites with the optimal connected filler network and with the excessive secondary filler. The nano-bridge effect and the suggested KJL model are expected to provide insights into the development of next-generation TIMs.

CRediT authorship contribution statement

Ji-un Jang: Writing – original draft, Data curation, Visualization. **Seung Hwan Lee:** Validation, Formal analysis. **Jaewoo Kim:** Methodology, Investigation. **Seong Yun Kim:** Conceptualization, Writing – review & editing, Project administration. **Seong Hun Kim:** Supervision.

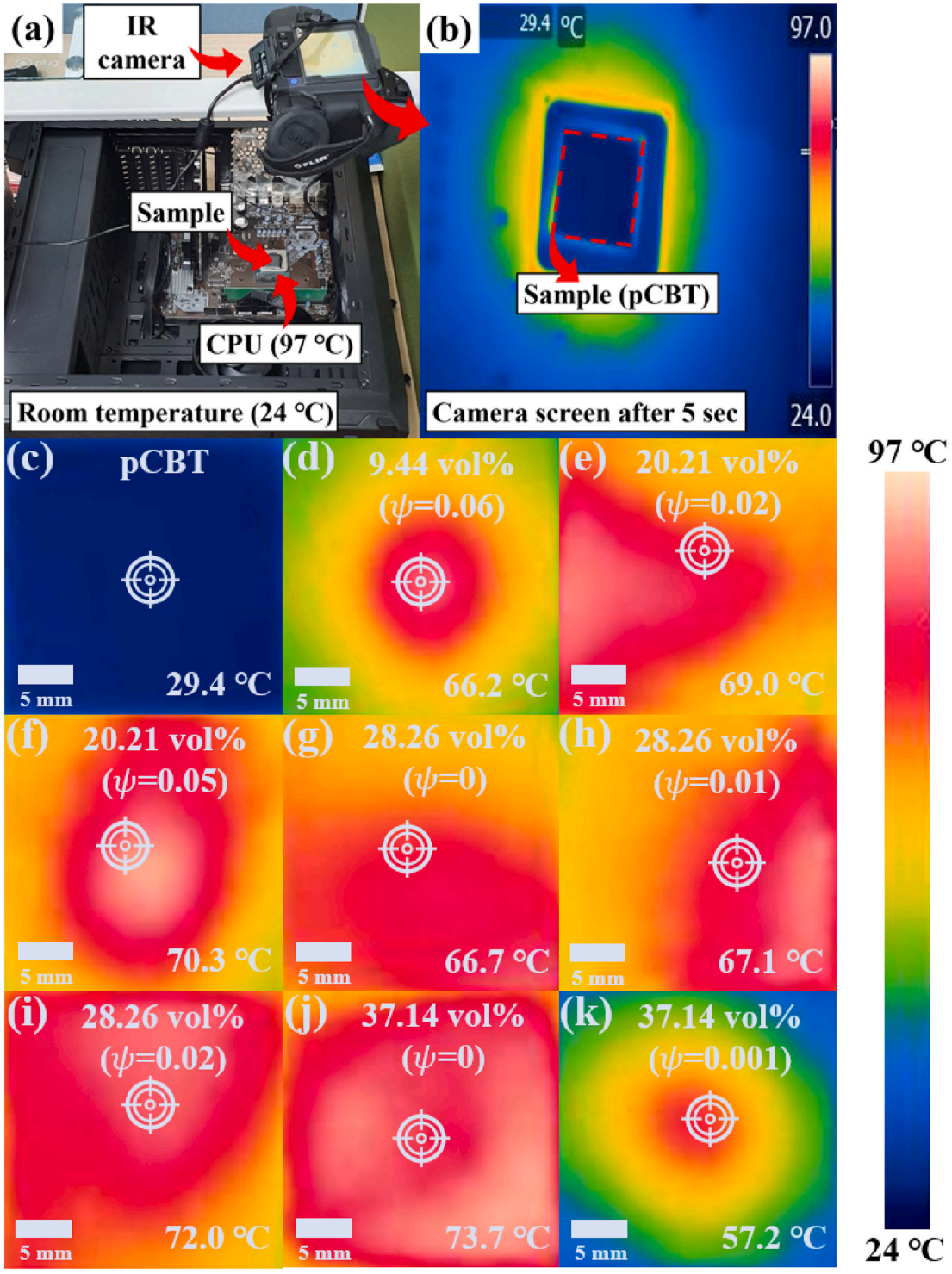

Fig. 4. (a) Photo image for IR thermal analysis and (b) screen image of IR camera after 5 s, and IR thermal images of the fabricated composites (c) without fillers, and filled with (d) 9.44 vol% GNP/MWCNT (ψ = 0.06), (e) 20.21 vol% GNP/MWCNT (ψ = 0.02), (f) 20.21 vol% GNP/MWCNT (ψ = 0.05), (g) 28.26 vol% GNP, (h) 28.26 vol% GNP/MWCNT (ψ = 0.01), (i) 28.26 vol% GNP/MWCNT (ψ = 0.02), (j) 37.14 vol% GNP and (k) 37.14 vol% GNP/MWCNT (ψ = 0.001).

Declaration of competing interest

The authors declare that they have no known competing financial interests or personal relationships that could have appeared to influence the work reported in this paper.

Acknowledgements

TEM images were obtained by aberration-corrected scanning transmission electron microscope (JEM-ARM200F, JEOL) in the Center for University-Wide Research Facilities(CURF) at Jeonbuk National University. This study was supported by Basic Science Research Program (2017R1C1B5077037) through the National Research Foundation of Korea (NRF) funded by the Ministry of Education and the Industrial

Technology Innovation Program (10082586) funded by the Ministry of Trade, Industry & Energy of Korea.

Appendix A. Supplementary data

Supplementary data to this article can be found online at https://doi.org/10.1016/j.compositesb.2021.109072.

References

[1] Iijima S. Helical microtubules of graphitic carbon. Nature 1991;354:56–8.
[2] Ebbesen TW, Lezec HJ, Hiura H, Bennett JW, Ghaemi HF, Thio T. Electrical conductivity of individual carbon nanotubes. Nature 1996;382:54–6.
[3] Kim P, Shi L, Majumdar A, EcEuen PL. Thermal transport measurements of individual multiwalled nanotubes. Phys Rev Lett 2001;87:215502.
[4] Yu C, Shi L, Yao Z, Li D, Majumdar A. Thermal conductance and thermopower of an individual single-wall carbon nanotube. Nano Lett 2005;5:1842–6.
[5] Novoselov KS, Geim AK, Morozov SV, Jiang D, Zhang Y, Dubonos SV, Grigorieva IV, Firsov AA. Electric field effect in atomically thin carbon films. Science 2004;306:666–9.
[6] Bolotin KI, Sikes KJ, Jiang Z, Klima M, Fudenberg G, Hone J, Kim P, Stormer HL. Ultrahigh electron mobility in suspended graphene. Solid State Commun 2008;146:351–5.
[7] Ghosh S, Calizo I, Teweldebrhan D, Pokatilov EP, Nika DL, Balandin AA, Bao W, Miao F, Lau CN. Extremely high thermal conductivity of graphene: prospects for thermal management applications in nanoelectronic circuits. Appl Phys Lett 2008;92:151911.
[8] Mora A, Verma P, Kumar S. Electrical conductivity of CNT/polymer composites: 3D printing, measurements and modeling. Compos B Eng 2020;183:107600.
[9] Fang Y, Li L-Y, Jang S-H. Calculation of electrical conductivity of self-sensing carbon nanotube composites. Compos B Eng 2020;199:108314.
[10] Chang E, Ameli A, Alian AR, Mark LH, Yu K, Wang S, Park CB. Percolation mechanism and effective conductivity of mechanically deformed 3-dimensional composite networks: computational modeling and experimental verification. Compos B Eng 2021;207:108552.
[11] Vertuccio L, Foglia F, Pantani R, Romero-Sánchez MD, Calderón B, Guadagno L. Carbon nanotubes and expanded graphite based bulk nanocomposites for de-icing applications. Compos B Eng 2021;207:108583.
[12] Guo B, Ji X, Wang W, Chen X, Wang P, Wang L, Bai J. Highly flexible, thermally stable, and static dissipative nanocomposite with reduced functionalized graphene oxide processed through 3D printing. Compos B Eng 2021;208:108598.
[13] Guo Y, Ruan K, Shi X, Yang X, Gu J. Factors affecting thermal conductivities of the polymers and polymer composites: a review. Compos Sci Technol 2020;193:108134.
[14] Han Z, Fina A. Thermal conductivity of carbon nanotubes and their polymer nanocomposites: a review. Prog Polym Sci 2011;36:914–44.
[15] Pak SY, Kim HM, Kim SY, Youn JR. Synergistic improvement of thermal conductivity of thermoplastic composites with mixed boron nitride and multi-walled carbon nanotube fillers. Carbon 2012;50:4830–8.
[16] Kim YG, Kim HS, Jo SM, Kim SY, Yang BJ, Cho J, Lee S, Cha JE. Thermally insulating, fire-retardant, smokeless and flexible polyvinylidene fluoride nanofibers filled with silica aerogels. Chem Eng J 2018;351:473–81.
[17] Shtein M, Nadiv R, Buzaglo M, Kahil K, Regev O. Thermally conductive graphene-polymer composites: size, percolation, and synergy effects. Chem Mater 2015;27:2100–6.
[18] Kim HS, Kim JH, Kim WY, Lee HS, Kim SY, Khil M-S. Volume control of expanded graphite based on inductively coupled plasma and enhanced thermal conductivity of epoxy composite by formation of the filler network. Carbon 2017;119:40–6.
[19] Yu A, Ramesh P, Sun X, Bekyarova E, Itkis ME, Haddon RC. Enhanced thermal conductivity in a hybrid graphite nanoplatelet–carbon nanotube filler for epoxy composites. Adv. Mater. 2008;20:4740–4.
[20] Seo H, Yun HD, Kwon S-Y, Bang IC. Hybrid graphene and single-walled carbon nanotube films for enhanced phase-change heat transfer. Nano Lett 2016;16:932–8.
[21] Huxtable ST, Cahill DG, Shenogin S, Xue L, Ozisik R, Barone P, Usrey M, Strano MS, Siddons G, Shim M, Keblinski P. Interfacial heat flow in carbon nanotube suspensions. Nat Mater 2003;2:731–4.
[22] Yang J, Waltermire S, Chen Y, Zinn AA, Xu TT, Li D. Contact thermal resistance between individual multiwall carbon nanotubes. Appl Phys Lett 2010;96:023109.
[23] Barani Z, Mohammadzadeh A, Geremew A, Huang C-Y, Coleman D, Mangolini L, Kargar F, Balandin AA. Thermal properties of the binary-filler hybrid composites with graphene and copper nanoparticles. Adv Funct Mater 2020;30:1904008.
[24] Kim HS, Bae HS, Yu J, Kim SY. Thermal conductivity of polymer composites with the geometrical characteristics of graphene nanoplatelets. Sci Rep 2016;6:26825.
[25] Jang J-u, Cha JE, Lee SH, Kim J, Yang B, Kim SY, Kim SH. Enhanced electrical and electromagnetic interference shielding properties of uniformly dispersed carbon nanotubes filled composite films via solvent-free process using ring-opening polymerization of cyclic butylene terephthalate. Polymer 2020;186:122030.
[26] Noh YJ, Joh H-I, Yu J, Hwang SH, Lee S, Lee CH, Kim SY, Youn JR. Ultra-high dispersion of graphene in polymer composite via solvent free fabrication and functionalization. Sci Rep 2015;5:9141.
[27] Jang J-u, Lee HS, Kim JW, Kim SY, Kim SH, Hwang I, Kang BJ, Kang MK. Facile and cost-effective strategy for fabrication of polyamide 6 wrapped multi-walled carbon nanotube via anionic melt polymerization of ε-caprolactam. Chem Eng J 2019;373:251–8.
[28] Abt T, Sánchez-Soto M. A review of the recent advances in cyclic butylene terephthalate technology and its composites. Crit. Rev. Solid State 2017;42:173–217.
[29] Jang J-u, Park HC, Lee HS, Khil M-S, Kim SY. Electrically and thermally conductive carbon fibre fabric reinforced polymer composites based on nanocarbons and an in situ polymerizable cyclic oligoester. Sci Rep 2018;8:7659.
[30] Nan C-W, Liu G, Lin Y, Li M. Interface effect on thermal conductivity of carbon nanotube composites. Appl Phys Lett 2004;85:3549.
[31] Stauffer D, Aharony A. Introduction to percolation theory. London: Taylor & Francis; 1992.
[32] Yu A, Ramesh P, Itkis ME, Bekyarova E, Haddon RC. Graphite nanoplatelet− epoxy composite thermal interface materials. J Phys Chem C 2007;111:7565–9.
[33] Huang X, Zhi C, Jiang P. Toward effective synergetic effects from graphene nanoplatelets and carbon nanotubes on thermal conductivity of ultrahigh volume fraction nanocarbon epoxy composites. J Phys Chem C 2012;116:23812–20.
[34] Che J, Wu K, Lin Y, Wang K, Fu Q. Largely improved thermal conductivity of HDPE/expanded graphite/carbon nanotubes ternary composites via filler network-network synergy. Compos. Part A Appl Sci Manuf 2017;99:32–40.
[35] Xiao YJ, Wang W-y, Chen X-j, Lin T, Zhang Y-t, Yang J-h, Wang Y, Zhou Z-w. Hybrid network structure and thermal conductive properties in poly(vinylidene fluoride) composites based on carbon nanotubes and graphene nanoplatelets. Compos. Part A Appl Sci Manuf 2016;90:614–25.
[36] Qi G-Q, Yang J, Bao R-Y, Liu Z-Y, Yang W, Xie B-H, Yang M-B. Enhanced comprehensive performance of polyethylene glycol based phase change material with hybrid graphene nanomaterials for thermal energy storage. Carbon 2015;88:196–205.
[37] Yang D, Xu H, Yu W, Wang J, Gong X. Dielectric properties and thermal conductivity of graphene nanoplatelet filled poly (vinylidene fluoride)(PVDF)/poly (methyl methacrylate)(PMMA) blend. J Mater Sci Mater Electron 2017;28:13006–12.
[38] Min C, Yu D, Cao J, Wang G, Feng L. A graphite nanoplatelet/epoxy composite with high dielectric constant and high thermal conductivity. Carbon 2013;55:116–25.
[39] He G, Zhou X, Liu J, Zhang J, Pan L, Liu S. Synergetic enhancement of thermal conductivity for highly explosive-filled polymer composites through hybrid carbon nanomaterials. Polym Compos 2018;39:1452–62.
[40] Zhao Y-H, Zhang Y-F, Bai SL. High thermal conductivity of flexible polymer composites due to synergistic effect of multilayer graphene flakes and graphene foam. Compos. Part A Appl Sci Manuf 2016;85:148–55.
[41] Yang J, Tang L-S, Bao R-Y, Bai L, Liu Z-Y, Yang W, Xie B-H, Yang M-B. Largely enhanced thermal conductivity of poly (ethylene glycol)/boron nitride composite phase change materials for solar-thermal-electric energy conversion and storage with very low content of graphene nanoplatelets. Chem Eng J 2017;315:481–90.
[42] Ramakrishnan S, Wang X, Sanjayan J. Thermal enhancement of paraffin/hydrophobic expanded perlite granular phase change composite using graphene nanoplatelets. Energy Build 2018;169:206–15.
[43] Prolongo SG, Moriche R, Del Rosario G, Jiménez-Suárez A, Prolongo MG, Ureña A. Joule effect self-heating of epoxy composites reinforced with graphitic nanofillers. J Polym Res 2016;23:189.
[44] Wang F, Drazal LT, Qin Y, Huang Z. Mechanical properties and thermal conductivity of graphene nanoplatelet/epoxy composites. J Mater Sci 2015;50:1082–93.
[45] Kong KTS, Mariatti M, Rashid AA, JJC Busfield. Enhanced conductivity behavior of polydimethylsiloxane (PDMS) hybrid composites containing exfoliated graphite nanoplatelets and carbon nanotubes. Compos B Eng 2014;58:457–62.
[46] Song P, Liu L, Fu S, Yu Y, Jin C, Wu Q, Zhang Y, Li Q. Striking multiple synergies created by combining reduced graphene oxides and carbon nanotubes for polymer nanocomposites. Nanotechnology 2013;24:125704.
[47] Zhang W-b, Zhang Z-x, Yang J-h, Huang T, Zhang N, Zheng X-t, Wang Y, Zhou Z-w. Largely enhanced thermal conductivity of poly (vinylidene fluoride)/carbon nanotube composites achieved by adding graphene oxide. Carbon 2015;90:242–54.
[48] Kumar S, Sun LL, Caceres S, Li B, Wood W, Perugini A, Maguire RG, Zhong WH. Dynamic synergy of graphitic nanoplatelets and multi-walled carbon nanotubes in polyetherimide nanocomposites. Nanotechnology 2010;21:105702.
[49] Yang S-Y, Lin W-N, Huang Y-L, Tien H-W, Wang J-Y, Ma C-CM, Li S-M, Wang Y-S. Synergetic effects of graphene platelets and carbon nanotubes on the mechanical and thermal properties of epoxy composites. Carbon 2011;49:793–803.
[50] Im H, Kim J. Thermal conductivity of a graphene oxide–carbon nanotube hybrid/epoxy composite. Carbon 2012;50:5429–40.
[51] Yu J, Choi HK, Kim HS, Kim SY. Synergistic effect of hybrid graphene nanoplatelet and multi-walled carbon nanotube fillers on the thermal conductivity of polymer composites and theoretical modeling of the synergistic effect. Compos. Part A Appl Sci Manuf 2016;88:79–85.
[52] Bigg DM. Thermal conductivity of heterophase polymer compositions. Adv Polym Sci 1995;119:1–30.